Structure of μ-Dinitrogen-bis(bis(pentamethylcyclopentadienyl)-dinitrogenzirconium(II)), $\{(\eta^5\text{-}C_5(CH_3)_5)_2ZrN_2\}_2N_2$

Robert D. Sanner, Juan M. Manriquez, Richard E. Marsh, and John E. Bercaw*

Contribution No. 5325 from the Arthur Amos Noyes Laboratory of Chemical Physics, California Institute of Technology, Pasadena, California 91125.
Received May 7, 1976

Abstract: The crystal structure of μ-dinitrogen-bis(bis(pentamethylcyclopentadienyl)dinitrogenzirconium(II)), $\{(\eta^5\text{-}C_5(CH_3)_5)_2ZrN_2\}_2N_2$, has been determined. The complex crystallizes in the monoclinic space group $P2_1/n$ with $a = 14.831$ (1), $b = 16.992$ (1), $c = 16.260$ (3) Å, $\beta = 90.00°$, and $Z = 4$; however, intimate twinning across the (100) or (001) mirror plane gives rise to an apparent orthorhombic diffraction symmetry. The structure factor, Fourier, and least-squares programs were therefore modified and full-matrix refinement converged at a final R index of 0.035 based on 4612 counter-collected data. The binuclear structure consists of two $(\eta^5\text{-}C_5Me_5)_2ZrN{\equiv}N$ moieties bridged by a third dinitrogen ligand. Terminal and bridging dinitrogen ligands are bound end-on to zirconium with essentially linear $ZrN{\equiv}N$ and $ZrN{\equiv}NZr$ arrangements. Terminal and bridging NN distances are 1.116 (8), 1.114 (7), and 1.182 (5) Å, respectively. A qualitative picture of the zirconium–dinitrogen bonding consistent with the structure and physical properties of the compound is presented.

Since their discovery ten years ago, over 100 transition metal compounds which contain molecular nitrogen (dinitrogen) as a ligand have been prepared.[1] However, these complexes have proven to be disappointingly inert with respect to reactions centered at N_2. During the same period several reaction systems involving transition metals have been developed which effectively reduce N_2 at room temperature and atmospheric pressure; however, no dinitrogen intermediates have been isolated from such reducing systems and hence their full structural characterization has not been possible. The nature of these "active" N_2 complex intermediates and their relationship to isolable, "inert" dinitrogen complexes have thus been subjects of considerable interest and speculation.

The relatively high efficiency of titanocene-based N_2 reducing systems has prompted numerous (unsuccessful) attempts to isolate a stable *crystalline* dinitrogen complex suitable for a structure determination.[2-6] In view of the difficulties associated with cyclopentadienyl-to-metal hydrogen transfer inherent to these systems, we have more recently investigated the closely related pentamethylcyclopentadienyl derivatives.[4,7-10] We find compounds containing the $(\eta^5\text{-}C_5Me_5)_2M$ (M = Ti, Zr) moiety often more stable and much more amenable to study than their $(\eta^5\text{-}C_5H_5)$ analogues. For example, in contrast to $\{(C_5H_5)_2Ti\}_2N_2$, $\{(C_5Me_5)_2Ti\}_2N_2$ is moderately stable in solution at room temperature and easily obtained as large, well-formed crystals.[9] The title compound $\{(C_5Me_5)_2ZrN_2\}_2N_2$ (**1**), is of comparable thermal stability and has also been isolated in crystalline form.[10] The unique spectral properties and the chemical reactivity associated with the coordinated N_2 in these complexes prompted us to examine their structures in some detail. This paper presents the results of an x-ray crystal structure determination for $\{(C_5Me_5)_2ZrN_2\}_2N_2$ and our interpretation of these results in terms of a plausible bonding scheme. An x-ray structure determination for $\{(C_5Me_5)_2Ti\}_2N_2$ appears in the following article.[11]

Experimental Section

$\{(C_5Me_5)_2ZrN_2\}_2N_2$ was prepared as described previously[10] and obtained as metallic green crystals from diethyl ether. A series of Weissenberg and precession photographs (Cu Kα and Mo Kα radiation) showed orthorhombic D_{2h}-*mmm* Laue symmetry with the systematic absences $h0l$, $h + l$ odd and $0k0$, k odd.

A crystal of dimensions 0.25 × 0.25 × 0.85 mm was mounted in a glass capillary under N_2 with its long axis (c) slightly skew to the ϕ axis of a G. E. XRD-5 quarter-circle diffractometer automated by Datex. Unit cell dimensions were obtained by a least-squares fit to the $(\sin^2\theta)/\lambda^2$ values measured on a diffractometer for ten reflections having high 2θ angles. Due to the extreme reactivity of the compound, an experimental density measurement was not attempted, although the calculated value of 1.31 g·cm^{-3} is a reasonable value for an organometallic compound of this type. Crystal data are given in Table I.

Intensities were measured for all hkl and $\overline{hkl}$ reflections between 4 and 153° in 2θ, using a θ–2θ scan technique and a scan of 2°/min; 20-s background counts were taken before and after each scan. The scan width varied linearly from 1.2° at $2\theta = 4°$ to 3.2° at $2\theta = 153°$. A variance $\sigma^2(I)$ was calculated for each reflection based on counting statistics and a term in $(0.02S)^2$, where S is the scan count. Intensities and their variances were corrected for Lorentz and polarization effects, while absorption corrections were made by the method of Wehe, Busing, and Levy using their ORABS program.[12] Intensities of three check reflections measured every 100 reflections indicated no crystal decomposition during data collection.

Intensities of reflections (hkl and $\overline{hkl}$ octants) were collected from which an averaged data set of 4803 intensities was assembled and placed on an absolute scale by means of a Wilson plot,[13] with scattering factors for all atoms calculated by the method of Cromer and Mann.[14] Systematic absences (177), six reflections which exceeded the counter capacity, and eight having an extremely unsymmetrical background were deleted, leaving 4612 reflections for the working data set.

Solution and Refinement. The systematic absences indicate an n-glide plane perpendicular to the b axis and a 2_1 screw axis parallel to the b axis. There is, however, no orthorhombic space group having this particular combination of symmetry elements, suggesting that one class of absences might be due to a pseudo-symmetry element. A three-dimensional Patterson map was generated, but attempted solution in several orthorhombic space groups containing one or the other of the observed symmetry elements proved futile.

The presence of either a (100) or a (001) twin plane operating on a monoclinic structure with $\beta = 90°$ and space group $P2_1/n$ would give rise to the apparent *mmm* diffraction symmetry, while the systematic absences characteristic of space group $P2_1/n$ would remain. Such twinning would have to be quite intimate, since there were no significant differences between the two octants of data and the Weissenberg and precession photographs showed no doubling of spots characteristic of twins.

Under these circumstances the intensity of a reflection may be expressed as the sum of the two equal twin contributors:

$$|G(hkl)|^2 = |G(\bar{h}kl)|^2 = |F(hkl)|^2 + |F(\bar{h}kl)|^2 \qquad (1)$$

Thus the orthorhombic Patterson map will represent a composite of the monoclinic twins and can be solved accordingly. Provided (as can be presumed for the centrosymmetric space group $P2_1/n$) that the

Table I. Crystal Data

$C_{40}H_{60}N_6Zr_2$	Monoclinic space group $P2_1/n$
a = 14.831 (1) Å	fw = 807.4
b = 16.992 (1) Å	ρ_{calcd} = 1.31 g·cm^{-3}
c = 16.260 (3) Å	Z = 4
β = 90.00°	μ = 47.0 cm^{-1}
V = 4098 Å^3	λ(Cu Kα) = 1.54178 Å

$F(hkl)$'s are real, eq 1 implies

$$|G(hkl)| = |F(hkl) + iF(\bar{h}kl)| \quad (2)$$

an expression which is analogous to the expression for the structure factor of an acentric crystal. We may define

$$|G(hkl)| = |A(hkl) + iB(\bar{h}kl)| \quad (3)$$

with

$$|A(hkl)| = |F(hkl)| \quad (4)$$

and

$$|B(\bar{h}kl)| = |F(\bar{h}kl)| \quad (5)$$

The structure-factor, Fourier, and least-squares programs were easily modified using eq 1–5. A somewhat similar treatment has been given previously by Wei for the structure determination of $Rh_4(CO)_{12}$.[15]

Zirconium positions obtained from the reinterpreted Patterson map led to an R index ($\Sigma||G_o| - |G_c||/\Sigma|G_o|$) of 0.307. Two successive structure-factor calculations interspersed with Fourier syntheses revealed the location of all remaining nonhydrogen atoms, yielding an R index of 0.165.

Refinement was by least-squares minimization of the quantity $\Sigma w|G_o^2 - s^2G_c^2|^2$, where $1/s$ is the scale factor for G_o and $w = 1/\sigma^2(G_o^2)$. In the initial least-squares cycles, positions and isotropic temperature factors for all nonhydrogen atoms, the scale factor, and a secondary extinction factor[16] were refined to an R index of 0.069. At this point, difference Fourier maps were generated in the planes of the methyl H atoms from which all 60 hydrogen atoms were located. Further full-matrix least-squares refinement was performed using two matrices, one containing coordinates for all nonhydrogen atoms and the other containing scale factor, secondary extinction factor, and anisotropic temperature factors for all nonhydrogen atoms. Isotropic thermal parameters for the hydrogen atoms were set approximately 1 Å^2 larger than those for their respective carbon atoms, but neither the thermal parameters nor coordinates of the hydrogen atoms were adjusted. Several least-squares cycles lowered the R index to 0.037, at which time the hydrogen atoms were repositioned on the basis of

Table II. Final Nonhydrogen Atom Parameters (coordinates × 10^5, U_{ij} × 10^4)[a,b,c]

Atom	X	Y	Z	U_{11}	U_{22}	U_{33}	U_{12}	U_{13}	U_{23}
Zr1	123 828 (2)	18 592 (2)	22 868 (3)	336 (2)	324 (2)	298 (2)	−2 (1)	−75 (2)	7 (1)
Zr2	87 925 (3)	16 516 (2)	24 155 (3)	331 (2)	462 (2)	383 (2)	−11 (1)	−67 (2)	0 (2)
N1	109 789 (24)	18 157 (18)	23 566 (28)	367 (18)	357 (16)	464 (24)	−15 (13)	−123 (18)	3 (16)
N2	101 869 (23)	17 512 (18)	23 986 (28)	330 (18)	354 (16)	448 (24)	13 (12)	−8 (18)	26 (17)
N3	122 166 (36)	17 908 (24)	9 520 (27)	768 (34)	535 (24)	295 (23)	101 (22)	−77 (22)	16 (17)
N4	121 397 (54)	17 327 (33)	2 720 (41)	1257 (60)	825 (40)	538 (40)	161 (37)	−27 (39)	−3 (29)
N5	89 709 (31)	3 736 (25)	24 109 (30)	646 (27)	570 (23)	464 (26)	−65 (20)	−107 (23)	−24 (22)
N6	90 327 (46)	−2 796 (29)	24 050 (44)	1277 (51)	545 (28)	880 (45)	−40 (30)	−215 (43)	−35 (31)
Cl	120 012 (29)	33 250 (23)	25 265 (38)	404 (22)	314 (18)	587 (33)	−40 (16)	−64 (23)	−35 (20)
C2	124 926 (36)	32 832 (24)	17 901 (34)	473 (27)	365 (22)	512 (31)	−60 (19)	−47 (25)	46 (18)
C3	133 857 (35)	30 095 (27)	19 886 (37)	438 (26)	398 (24)	605 (35)	−52 (19)	−32 (24)	15 (22)
C4	134 217 (32)	28 972 (27)	28 451 (35)	422 (25)	429 (22)	560 (33)	−72 (19)	−147 (23)	4 (22)
C5	125 625 (35)	30 644 (25)	31 877 (32)	495 (27)	375 (22)	489 (29)	−84 (20)	−93 (25)	−65 (19)
C6	110 681 (33)	36 443 (27)	26 061 (44)	465 (25)	425 (22)	867 (43)	35 (19)	−50 (30)	−131 (28)
C7	121 782 (43)	35 957 (32)	9 830 (39)	736 (38)	485 (27)	599 (38)	−68 (26)	−115 (31)	154 (26)
C8	141 556 (44)	29 794 (37)	13 889 (52)	553 (36)	641 (37)	938 (56)	−70 (28)	160 (36)	6 (36)
C9	142 758 (40)	28 146 (36)	33 459 (48)	556 (35)	600 (33)	952 (52)	−89 (26)	−405 (35)	−16 (34)
C10	123 536 (50)	30 872 (34)	40 906 (40)	804 (42)	647 (34)	571 (36)	−111 (32)	−102 (36)	−134 (28)
C11	136 289 (31)	8 481 (25)	26 027 (37)	414 (22)	414 (22)	696 (37)	42 (17)	−120 (25)	27 (24)
C12	131 856 (36)	6 052 (29)	18 842 (35)	494 (26)	442 (26)	517 (32)	77 (21)	−13 (24)	35 (23)
C13	122 805 (33)	4 062 (25)	20 839 (30)	500 (25)	333 (19)	457 (28)	21 (19)	−138 (22)	14 (18)
C14	121 750 (31)	5 229 (27)	29 341 (33)	386 (23)	408 (23)	524 (30)	44 (18)	−17 (21)	109 (21)
C15	130 004 (37)	8 084 (30)	32 603 (36)	584 (30)	434 (25)	514 (33)	43 (22)	−202 (26)	4 (23)
C16	146 271 (35)	9 584 (35)	26 872 (57)	388 (25)	641 (32)	1389 (70)	55 (22)	−148 (40)	15 (44)
C17	136 395 (53)	4 742 (39)	10 735 (47)	884 (50)	716 (38)	734 (48)	264 (37)	125 (42)	24 (35)
C18	115 916 (43)	289 (30)	15 368 (46)	715 (39)	426 (27)	920 (51)	−36 (26)	−397 (37)	−63 (30)
C19	113 474 (44)	2 992 (36)	34 062 (46)	611 (36)	640 (35)	874 (49)	96 (30)	118 (36)	332 (34)
C20	131 951 (58)	9 466 (40)	41 513 (43)	1244 (64)	693 (39)	557 (41)	70 (41)	−419 (44)	3 (33)
C21	75 734 (41)	18 972 (44)	13 385 (38)	413 (29)	1153 (52)	470 (33)	−2 (33)	−40 (27)	95 (33)
C22	80 270 (43)	12 200 (38)	11 101 (40)	652 (37)	756 (39)	547 (38)	−230 (31)	−265 (31)	101 (31)
C23	89 359 (35)	14 357 (32)	8 953 (34)	467 (29)	602 (29)	454 (30)	76 (24)	−109 (24)	−16 (24)
C24	89 991 (36)	22 511 (31)	10 111 (33)	486 (28)	571 (29)	436 (30)	−30 (23)	−162 (24)	38 (23)
C25	81 655 (44)	25 432 (37)	12 836 (37)	710 (39)	700 (37)	450 (33)	230 (30)	−159 (30)	−10 (28)
C26	65 596 (54)	19 459 (78)	14 105 (60)	483 (41)	3269 (165)	669 (59)	207 (64)	−251 (40)	49 (75)
C27	76 025 (70)	4 212 (49)	9 653 (53)	1533 (86)	1055 (56)	811 (57)	−713 (61)	−528 (60)	88 (46)
C28	96 030 (55)	9 087 (43)	5 020 (42)	1001 (55)	910 (46)	560 (40)	412 (43)	−159 (40)	−103 (35)
C29	98 068 (50)	27 443 (45)	7 665 (45)	820 (46)	1006 (48)	585 (42)	−333 (40)	−193 (37)	281 (38)
C30	79 028 (79)	33 897 (47)	14 009 (53)	1791 (99)	868 (50)	645 (50)	696 (58)	−81 (57)	65 (39)
C31	91 366 (35)	19 916 (36)	39 393 (38)	356 (24)	780 (38)	483 (34)	−19 (24)	−6 (23)	−19 (28)
C32	86 962 (37)	12 597 (33)	39 309 (34)	454 (28)	686 (33)	455 (31)	−10 (25)	−28 (25)	41 (25)
C33	78 074 (37)	13 680 (38)	36 253 (36)	467 (29)	809 (38)	433 (31)	−90 (27)	−32 (24)	13 (28)
C34	77 056 (36)	21 755 (37)	34 652 (35)	398 (27)	808 (36)	484 (32)	100 (26)	−40 (24)	−85 (27)
C35	85 410 (38)	25 591 (33)	36 286 (34)	557 (32)	611 (31)	410 (30)	0 (25)	−2 (24)	−82 (24)
C36	100 689 (39)	21 453 (44)	42 677 (39)	447 (29)	1188 (51)	412 (33)	−111 (33)	−67 (26)	−141 (34)
C37	90 516 (49)	5 104 (45)	43 132 (44)	778 (44)	1001 (51)	602 (42)	35 (39)	2 (36)	311 (39)
C38	70 704 (49)	7 594 (50)	36 247 (49)	661 (41)	1158 (81)	724 (50)	−334 (40)	33 (37)	52 (46)
C39	68 134 (44)	25 759 (52)	33 325 (47)	511 (33)	1387 (65)	679 (47)	260 (38)	−59 (34)	−135 (47)
C40	86 993 (58)	34 308 (38)	36 296 (47)	965 (53)	642 (35)	718 (46)	−3 (37)	97 (45)	−125 (33)

[a] The final value of the scale factor is 0.7537 (16). [b] The final value of the secondary extinction factor is 1.13 (6) × 10^{-6}. [c] The form of the anisotropic temperature factor is $\exp[-2\pi^2(h^2a^{*2}u_{11} + \ldots + 2klb^*c^*u_{23})]$.

Table III. Final Hydrogen Atom Parameters (coordinates × 10^4)[a]

Atom	X	Y	Z	B
H6A	10 907	3664	3175	5.13
H6B	11 040	4166	2380	5.13
H6C	10 652	3310	2318	5.13
H7A	12 165	4151	1002	5.50
H7B	12 566	3427	574	5.50
H7C	11 582	3391	869	5.50
H8A	14 607	2616	1592	5.89
H8B	13 950	2787	880	5.89
H8C	14 422	3485	1332	5.89
H9A	14 134	2544	3855	5.88
H9B	14 711	2532	3051	5.88
H9C	14 501	3336	3486	5.88
H10A	12 567	3562	4328	6.13
H10B	11 721	3054	4182	6.13
H10C	12 641	2652	4370	6.13
H16A	14 902	476	2812	6.71
H16B	14 866	1156	2181	6.71
H16C	14 748	1326	3116	6.71
H17A	13 966	−7	1090	6.80
H17B	13 201	446	651	6.80
H17C	14 025	898	948	6.80
H18A	11 051	331	1562	5.71
H18B	11 811	18	1001	5.71
H18C	11 478	−481	1727	5.71
H19A	11 413	446	3957	6.01
H19B	10 852	530	3159	6.01
H19C	11 272	−270	3361	6.01
H20A	12 638	992	4449	6.54
H20B	13 540	520	4364	6.54
H20C	13 514	1417	4221	6.54
H26A	6 346	1539	1770	8.94
H26B	6 375	2436	1581	8.94
H26C	6 284	1834	868	8.94
H27A	7 258	285	1442	8.00
H27B	7 206	464	511	8.00
H27C	8 050	40	875	8.00
H28A	9 513	383	674	7.07
H28B	9 557	954	−88	7.07
H28C	10 201	1081	637	7.07
H29A	10 326	2547	1014	6.65
H29B	9 855	2743	188	6.65
H29C	9 699	3278	927	6.65
H30A	7 649	3469	1926	7.39
H30B	8 407	3715	1331	7.39
H30C	7 458	3536	995	7.39
H36A	10 076	2616	4573	6.04
H36B	10 243	1714	4618	6.04
H36C	10 501	2120	3832	6.04
H37A	8 855	481	4855	6.51
H37B	8 813	73	4011	6.51
H37C	9 688	506	4281	6.51
H38A	6 693	828	4081	6.27
H38B	6 731	794	3138	6.27
H38C	7 351	233	3659	6.27
H39A	6 586	2752	3845	7.04
H39B	6 910	3021	2978	7.04
H39C	6 414	2231	3067	7.04
H40A	8 705	3620	4179	6.19
H40B	9 257	3541	3376	6.19
H40C	8 226	3688	3322	6.19

[a] Thermal parameters are of the form exp $[-B((\sin^2\theta)/\lambda^2)]$.

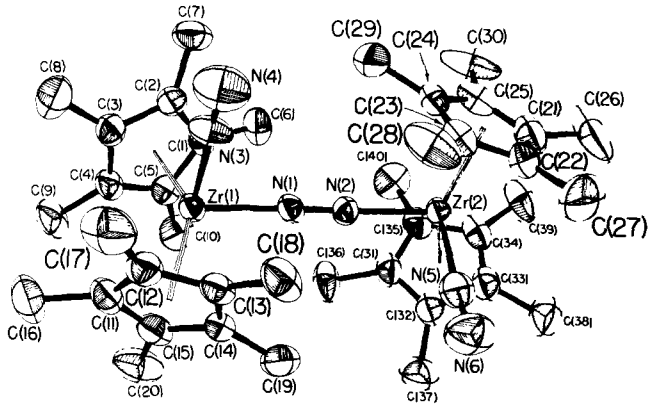

Figure 1. The molecular configuration of $[(\eta^5\text{-}C_5(CH_3)_5)_2ZrN_2]_2N_2$. In this and subsequent figures, thermal ellipsoids are drawn at the 50% probability level.

Table IV. Bond Distances (Å)

Zr1–N1	2.087 (3)	C1–C6	1.492 (7)
Zr1–N3	2.188 (4)	C2–C7	1.490 (7)
Zr2–N2	2.075 (3)	C3–C8	1.502 (8)
Zr2–N5	2.188 (4)	C4–C9	1.512 (8)
N1–N2	1.182 (5)	C5–C10	1.501 (8)
N3–N4	1.116 (8)	C11–C12	1.403 (7)
N5–N6	1.114 (7)	C12–C13	1.422 (7)
Zr1–R1[a]	2.232 (4)	C13–C14	1.405 (6)
Zr1–R2[a]	2.232 (5)	C14–C15	1.420 (7)
Zr2–R3[a]	2.229 (5)	C15–C11	1.420 (7)
Zr2–R4[a]	2.237 (5)	C11–C16	1.499 (8)
Zr1–C1	2.584 (4)	C12–C17	1.497 (9)
Zr1–C2	2.556 (4)	C13–C18	1.499 (7)
Zr1–C3	2.504 (5)	C14–C19	1.497 (8)
Zr1–C4	2.512 (5)	C15–C20	1.496 (9)
Zr1–C5	2.532 (4)	C21–C22	1.384 (9)
Zr1–C11	2.575 (4)	C22–C23	1.440 (8)
Zr1–C12	2.527 (5)	C23–C24	1.401 (7)
Zr1–C13	2.495 (4)	C24–C25	1.404 (8)
Zr1–C14	2.522 (4)	C25–C21	1.409 (9)
Zr1–C15	2.556 (5)	C21–C26	1.510 (12)
Zr2–C21	2.551 (6)	C22–C27	1.515 (11)
Zr2–C22	2.516 (6)	C23–C28	1.480 (9)
Zr2–C23	2.508 (5)	C24–C29	1.515 (9)
Zr2–C24	2.519 (5)	C25–C30	1.502 (11)
Zr2–C25	2.559 (6)	C31–C32	1.405 (8)
Zr2–C31	2.595 (5)	C32–C33	1.421 (8)
Zr2–C32	2.556 (5)	C33–C34	1.405 (8)
Zr2–C33	2.497 (5)	C34–C35	1.425 (8)
Zr2–C34	2.511 (5)	C35–C31	1.402 (8)
Zr2–C35	2.531 (5)	C31–C36	1.505 (8)
C1–C2	1.404 (6)	C32–C37	1.512 (9)
C2–C3	1.441 (7)	C33–C38	1.505 (9)
C3–C4	1.407 (7)	C34–C39	1.504 (9)
C4–C5	1.420 (6)	C35–C40	1.500 (9)
C5–C1	1.430 (6)		

[a] R1 = C1–C5 ring centroid, R2 = C11–C15 ring centroid, R3 = C21–C25 ring centroid, R4 = C31–C35 ring centroid.

another set of difference Fourier maps. Two final least-squares cycles led to an R index of 0.035 and a goodness of fit, $\{\Sigma w(G_o^2 - s^2G_c^2)/(N - P)\}^{1/2}$, of 3.42 for $N = 4612$ reflections and $P = 434$ parameters. All crystallographic computations were performed under the CRYM system[17] on an IBM 370/158 computer. Final parameters are given in Tables II and III.

Results and Discussion

The molecular structure is shown in Figure 1, a stereoscopic view in Figure 2, and the packing of the molecules in the unit cell is illustrated in Figure 3. The binuclear structure may be viewed as two $(\eta^5\text{-}C_5Me_5)_2ZrN{\equiv}N$ moieties bridged by a third dinitrogen ligand. Of special significance is the fact that the terminal and bridging dinitrogen ligands are bound *end-on* (η^1-) to zirconium with essentially linear ZrN≡N and ZrN≡NZr arrangements.

The skeletal view shown in Figure 4 illustrates the roughly tetrahedral disposition of $(\eta^5\text{-}C_5Me_5)$ and dinitrogen ligands about Zr, although substantial distortions do exist. Thus the centroid-Zr-centroid angles (R-Zr-R; Table V) average 141.3 (3)°, while the N-Zr-N angles average 87.1 (8)°.[18] The R-Zr-R angle is larger and the N-Zr-N angle somewhat smaller than found for similar molecules containing unsubstituted C_5H_5 rings, where the corresponding angles are 128

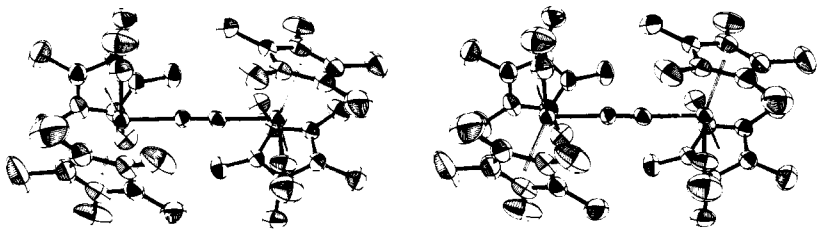

Figure 2. Stereoscopic view of $\{(\eta^5\text{-}C_5(CH_3)_5)_2ZrN_2\}_2N_2$.

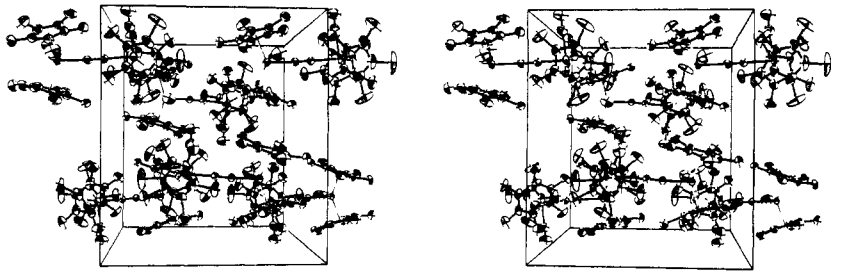

Figure 3. Stereoscopic view of the packing of the molecules in the unit cell. Positive x runs from left to right, positive y from bottom to top, positive z from back to front.

Table V. Bond Angles (deg)

Zr1–N1–N2	176.7 (3)	C11–C12–C17	124.5 (5)
Zr1–N3–N4	177.9 (5)	C13–C12–C17	126.2 (5)
Zr2–N2–N1	177.4 (3)	C12–C13–C18	127.6 (5)
Zr2–N5–N6	177.8 (5)	C14–C13–C18	124.6 (4)
N1–Zr1–N3	86.5 (2)	C13–C14–C19	124.0 (5)
R1–Zr1–R2	141.5 (2)	C15–C14–C19	127.0 (5)
R1–Zr1–N1	106.6 (2)	C11–C15–C20	126.5 (5)
R1–Zr1–N3	102.2 (2)	C14–C15–C20	125.6 (5)
R2–Zr1–N1	105.6 (2)	C21–C22–C23	108.0 (5)
R2–Zr1–N3	100.3 (2)	C22–C23–C24	106.4 (5)
N2–Zr2–N5	87.7 (2)	C23–C24–C25	109.5 (5)
R3–Zr2–R4	141.1 (2)	C24–C25–C21	107.1 (5)
R3–Zr2–N2	105.9 (2)	C25–C21–C22	109.1 (6)
R3–Zr2–N5	101.4 (2)	C22–C21–C26	123.4 (7)
R4–Zr2–N2	105.9 (2)	C25–C21–C26	125.6 (6)
R4–Zr2–N5	101.6 (2)	C21–C22–C27	125.8 (6)
C1–C2–C3	107.6 (4)	C23–C22–C27	125.4 (6)
C2–C3–C4	107.5 (4)	C22–C23–C28	125.2 (5)
C3–C4–C5	109.1 (4)	C24–C23–C28	127.7 (5)
C4–C5–C1	106.8 (4)	C23–C24–C29	124.4 (5)
C5–C1–C2	108.9 (4)	C25–C24–C29	125.7 (5)
C2–C1–C6	125.0 (4)	C21–C25–C30	125.2 (6)
C5–C1–C6	126.0 (4)	C24–C25–C30	127.4 (6)
C1–C2–C7	124.8 (5)	C31–C32–C33	108.7 (5)
C3–C2–C7	126.9 (5)	C32–C33–C34	106.9 (5)
C2–C3–C8	124.4 (5)	C33–C34–C35	108.6 (5)
C4–C3–C8	127.5 (5)	C34–C35–C31	107.5 (5)
C3–C4–C9	125.3 (5)	C35–C31–C32	108.2 (5)
C5–C4–C9	124.0 (5)	C32–C31–C36	125.8 (5)
C1–C5–C10	127.4 (5)	C35–C31–C36	126.0 (5)
C4–C5–C10	125.1 (5)	C31–C32–C37	125.4 (5)
C11–C12–C13	108.8 (4)	C33–C32–C37	125.2 (5)
C12–C13–C14	107.2 (4)	C32–C33–C38	125.8 (6)
C13–C14–C15	108.6 (4)	C34–C33–C38	126.4 (6)
C14–C15–C11	107.5 (4)	C33–C34–C39	124.3 (6)
C15–C11–C12	107.8 (4)	C35–C34–C39	125.8 (5)
C12–C11–C16	125.2 (5)	C31–C35–C40	125.5 (5)
C15–C11–C16	125.8 (5)	C34–C35–C40	126.0 (5)

Table VI. Least-Squares Planes of Cyclopentadienyl Rings

Atom	Deviation, Å[b]	Atom	Deviation, Å[b]
	Ring 1 (α = 2.2°)[a]		Ring 2 (α = 2.0°)[a]
C1	0.012	C11	0.004
C2	−0.002	C12	0.000
C3	−0.008	C13	−0.005
C4	0.015	C14	0.008
C5	−0.016	C15	−0.008
C6	0.134	C16	0.273
C7	0.185	C17	0.168
C8	0.149	C18	0.152
C9	0.366	C19	0.153
C10	0.127	C20	0.109
	Ring 3 (α = 1.6°)[a]		Ring 4 (α = 2.7°)[a]
C21	0.002	C31	0.011
C22	−0.003	C32	0.001
C23	0.002	C33	−0.013
C24	−0.001	C34	0.020
C25	−0.001	C35	−0.019
C26	0.327	C36	0.113
C27	0.200	C37	0.202
C28	0.200	C38	0.164
C29	0.161	C39	0.352
C30	0.138	C40	0.153

[a] Tilt angle α = angle defined by the intersection of the Zr–ring centroid vector with the normal to the cyclopentadienyl ring plane. [b] A positive deviation is a deviation away from Zr.

and 96° for $(\eta^5\text{-}C_5H_5)_2ZrF_2$,[19] 126 and 96° for $(\eta^5\text{-}C_5H_5)_2ZrI_2$,[19] and 130 and 94° for $(\eta^5\text{-}C_5H_5)_2ZrCl\{Si(C_6H_5)_3\}$;[20] 134 and 95° for $(\eta^5\text{-}C_5H_5)_2TiS_5$,[21] 130 and 86° for $(\eta^5\text{-}C_5H_5)_2Ti(\eta^1\text{-}C_5H_5)_2$,[22] and 130 and 95° for $(\eta^5\text{-}C_5H_5)_2TiCl_2$.[23] It appears that steric crowding of the methyl groups between rings is responsible for the expansion of the R-Zr-R angles for **1**, so that the arrangement of ligands more closely resembles that for $\{\eta^5\text{-}C_5(CH_3)_5\}_2TiCl_2$, where the R-Ti-R and Cl-Ti-Cl angles are 137 and 93°, respectively.[24] The R-Zr-terminal nitrogen and R-Zr-bridging nitrogen angles are more nearly equal, averaging 101.4 (8) and 106.0 (4)°, respectively.

Metal–Ring Bonding. The cyclopentadienyl rings are nearly planar (Table VI). Zr-R (2.232 (3) Å) and Zr-ring C distances (2.54 (3) Å) are not unlike those found for $(\eta^5\text{-}C_5H_5)_nZrX_{4-n}$ (n = 1, 2) derivatives.[19,20,25-27] The symmetrical metal-to-ring bonding is most evident from the Zr-C distances, which fall in the narrow range 2.495-2.595 Å; small tilts of all four rings with respect to the Zr-ring centroid vector (Table VI) account for the variations in these bond lengths. The average $(C\text{-}C)_{ring}$ bond length of 1.413 (14) Å is nearly identical with that found for $\{\eta^5\text{-}C_5(CH_3)_5\}_2TiCl_2$ (1.409 (13) Å)[24] and within the range found for $(\eta^5\text{-}C_5H_5)_nZrX_{4-n}$ (n =

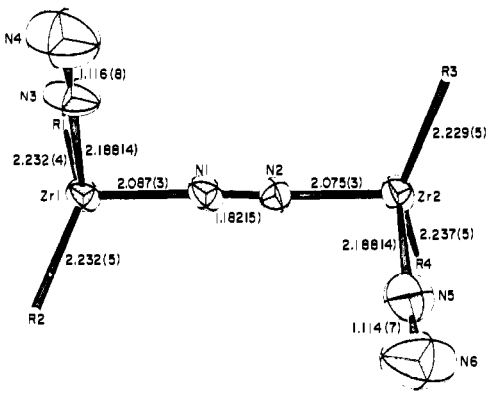

Figure 4. Skeletal view of $\{(\eta^5\text{-}C_5(CH_3)_5)_2ZrN_2\}_2N_2$.

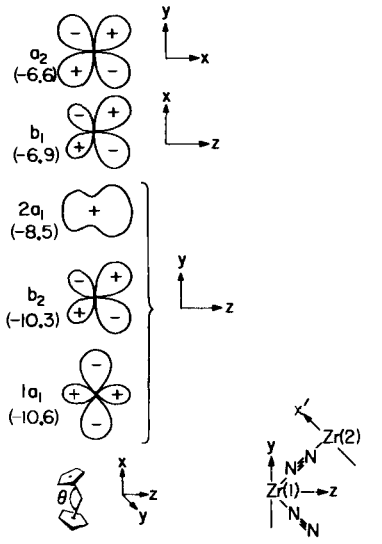

Figure 5. Contours of the five frontier orbitals of a bent, eclipsed $(\eta^5\text{-}C_5H_5)_2M$ fragment. Approximate energies (eV) from ref 36 for $\theta = 141°$ are given in parentheses.

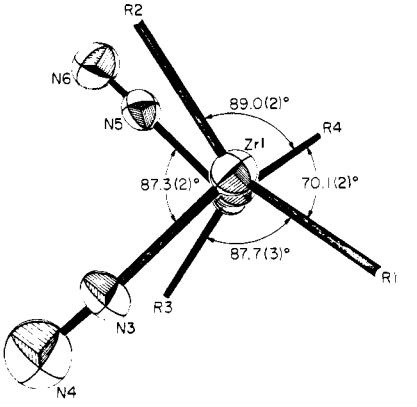

Figure 6. Skeletal view down the Zr-Zr axis revealing torsion angles.

1, 2) derivatives. Although these $(C\text{-}C)_{ring}$ distances vary from 1.384 to 1.441 Å with individual esd's of 0.009 Å, this variation is probably not significant, so that all four $\{C_5(CH_3)_5\}$ rings may be considered bonded to the zirconium atoms in a true *pentahapto* fashion.

As shown in Table VI, all methyl groups are bent out of their respective cyclopentadienyl planes away from zirconium. Methyl-methyl contacts between rings, as observed previously for the structure of $(\eta^5\text{-}C_5Me_5)_2TiCl_2$,[24] may be cited to explain the variations of these deviations. Thus the two shortest inter-ring C···C nonbonded distances are observed for C9-C16 (3.371 (9) Å) and C26-C39 (3.325 (9) Å), and accordingly these four carbon atoms exhibit the greatest deviations from their ring planes. All other inter-ring C···C contacts exceed 3.7 Å. Close contacts between the methyl and terminal N_2 groups prevent two rings bonded to a single zirconium atom from being strictly staggered. Appreciable CH_3-N crowding appears to remain, however, resulting in deviations from planarity for several other methyl groups in the molecule. Thus C7-N3, C17-N3, C37-N5, and C27-N5 contacts of 3.068 (8), 3.082 (9), 3.104 (8), and 3.106 (8) Å, respectively, lead to substantial deviations of these methyl groups from ring planarity.

Metal Dinitrogen Bonding. **1** appears to represent the only structurally characterized compound of zirconium(II), so that a strict comparison of Zr-N bond lengths of **1** to other Zr(II) complexes cannot be made. Three x-ray crystal structures for Zr(IV) complexes which contain N-bound ligands have been reported however. An unusually long Zr-N distance of 2.539 (8) Å was observed for the eight-coordinate complex tetrakis(*N*-ethylsalicylaldimato)zirconium(IV).[28] A similar, but somewhat shorter value of 2.439 (9) Å has been reported for the dodecahedral $Zr[N(CH_2COO)_3]_2^{2-}$ ion.[29] The two Zr-N distances of 2.110 (5) and 2.124 (5) Å observed for $(\eta^5\text{-}C_5H_5)_2Zr(NCO)_2$[30] compare more favorably to those for **1** (2.188 (4), 2.188 (4), 2.087 (3), and 2.075 (3) Å).

The conventional end-on bonding mode established herein for both terminal and bridging dinitrogen ligands is of special significance in light of several earlier suggestions that either an edge-on[4,8,9] or doubly bent (azo)[3] coordination should be favored for complexes of this type. The two terminal N-N bond lengths (1.116 (8) and 1.114 (7) Å) are the same as those found previously for other mononuclear dinitrogen complexes (1.11 ± 0.01 Å),[1] only slightly expanded from that for free N_2 (1.0976 Å). The bridging dinitrogen ligand, however, exhibits a significantly longer N-N distance (1.182 (5) Å), indicative of a substantial reduction in bond order.

A qualitative description of the $Zr\text{-}N_2$ bonding may be formulated by suitable combinations of dinitrogen lone pair, π, and π^* orbitals with those of the bent bis(η^5-cyclopentadienyl)zirconium(II) fragments. With respect to the latter, several theoretical and experimental papers have examined the shapes and energies of the frontier orbitals of a bent $(\eta^5\text{-}C_5H_5)_2M$ unit.[31-35] Figure 5 shows these orbitals as recently reported by Lauher and Hoffmann for an eclipsed-ring geometry (C_{2v} symmetry). If it is assumed that eclipsed and staggered configurations are of similar energies and also that substitution of methyl groups for the ten cyclopentadienyl hydrogens exerts no major effects, then for $\theta = 141°$ the energies of these five frontier orbitals are approximately as shown.[36] The three low-lying orbitals have significant extent in the *yz* plane; the b_2 orbital is chiefly d_{yz} in character; the two a_1 orbitals each contain some contribution from s and p_z orbitals in addition to $d_{x^2-y^2}$ and d_{z^2}.

As can be seen orbitals b_2 and $2a_1$ are of proper symmetry for interaction with both terminal and bridging dinitrogen lone-pair orbitals. π bonding is also possible utilizing N_2 π^* acceptor orbitals and the filled $1a_1$ orbital of zirconium. As shown in Figure 6, the N3-Zr···Zr-N5 torsion angle of 87.3 (2)° (Table VII) approximates that expected for interaction of one of the bridging N_2 π^* acceptor orbitals with the filled $1a_1$ orbital of Zr(1), the other with the corresponding electron pair on Zr(2). This favorable bonding situation undoubtedly contributes to the greater overall stability of the gauche configuration of the dimer relative to the cis or trans forms and results in additional weakening of the N≡N bond of the N_2 bridge.

An important feature of the $(ZrN{\equiv}N)_2N_2$ substructure requiring closer scrutiny is the fact that the two Zr-N distances for the bridge (2.087 (3) and 2.075 (3) Å) are significantly shorter than those for the terminal dinitrogen-zirconium bonds

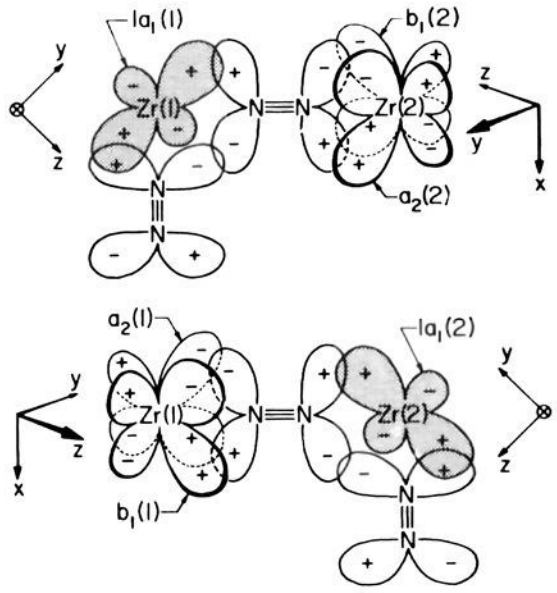

Figure 7. Interactions of N_2 π^* orbitals with $1a_1$, b_1, and a_2 zirconium orbitals. Coordinate systems for Zr(1) and Zr(2) are defined separately; labels for metal orbitals are for idealized local C_{2v} symmetry. The b_1 and a_2 orbitals are directed 45° from plane of paper.

Table VII. Torsion Angles

Atom 1	Atom 2	Atom 3	Atom 4	Angle, deg[a]
N3	Zr1	Zr2	N5	87.3 (2)
N3	Zr1	Zr2	R3	−13.7 (2)
N3	Zr1	Zr2	R4	−171.5 (2)
R1	Zr1	Zr2	N5	−171.3 (2)
R1	Zr1	Zr2	R3	87.7 (2)
R1	Zr1	Zr2	R4	−70.1 (2)
R2	Zr1	Zr2	N5	−12.2 (2)
R2	Zr1	Zr2	R3	−113.2 (2)
R2	Zr1	Zr2	R4	89.0 (2)

[a] Looking from atom 2 to atom 3, the angle of clockwise rotation for bond 3–4 with reference to bond 1–2.

(2.188 (4) and 2.188 (4) Å). On the basis of zirconium-to-dinitrogen back-bonding *alone*, it is difficult to reconcile a higher Zr–dinitrogen bond order for the bridge. Population of an N_2 π^* orbital by the $1a_1$ electron pair of one zirconium with its consequent charge buildup on the bridging N_2 can only oppose donation of electron density from the other zirconium into the orthogonal N_2 π^* orbital. There must therefore exist a bonding mechanism by which this charge buildup on the N_2 bridge is relieved. While one may cite a synergetic σ donation of the N_2 lone pair into empty b_1 and/or $2a_1$ zirconium orbitals, we favor an interaction which allows this charge buildup to be delocalized into empty π-type orbitals of a second Zr center (Figure 7). As can be seen the relative orientation of Zr(2) with respect to Zr(1) results in wedging of nitrogen p orbitals between empty b_1 and a_2 π-type orbitals.[37] This interaction thus allows delocalization of $1a_1$ electron density from Zr(1) into empty N_2 π^* orbitals, and further, allows for donation of μ-N_2 π-electron density into b_1 and a_2 acceptor orbitals of Zr(2).

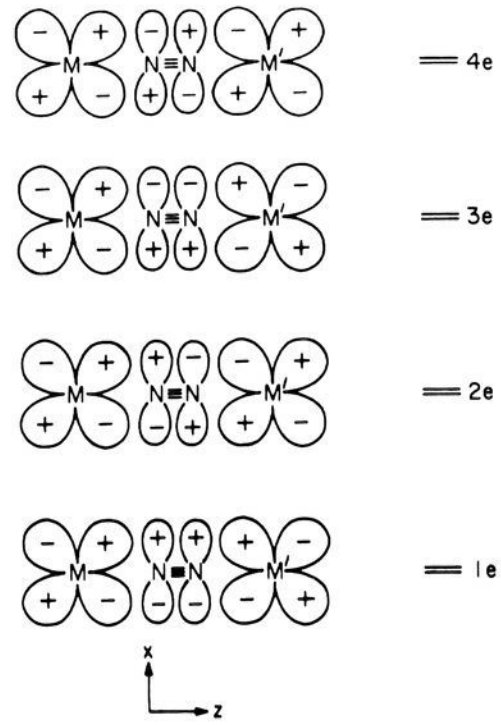

Figure 8. Qualitative four-center molecular orbital scheme for binuclear dinitrogen complexes in idealized C_{4v} symmetry. Shown is one of the two equivalent π-type orbitals only. Ordering of levels is that proposed in ref 43.

The symmetry of the molecule demands an equivalent, opposing "push–pull" interaction from Zr(2) to Zr(1) utilizing the orthogonal N_2 π and π^* orbitals of the bridge.

Infrared spectra for **1** are in accord with strong electronic coupling of the two zirconium centers. KBr pellet spectra exhibit three bands (2040 (s), 2003 (vs), and 1578 cm^{-1} (m)) attributable to N–N stretching modes.[10,38] Apart from the exceptionally low frequency for one of the bands, two features of the spectrum were rather unexpected: (i) in view of the nearly orthogonal spatial relationship of the two terminal N_2's, the observation of *two* terminal N–N stretching frequencies requires substantial electronic (rather than through-space dipolar) coupling of these vibrations; and (ii) the intensity of the bridging N–N stretching mode is much higher than would be expected considering the symmetry of the dimer. Both features are reconciled, however, if the spectrum is interpreted on the basis of a coupling of the symmetric combination of terminal N–N stretches (2040 cm^{-1}) with the bridging N–N mode (1578 cm^{-1}), the latter gaining intensity from the former. The strongest band (2003 cm^{-1}) may then be attributed to the antisymmetric combination of terminal N–N stretching modes. Such coupling of bridge and terminal N_2 stretching modes is indeed expected, since both terminal and bridging dinitrogens compete for the same zirconium $1a_1$ electron pair density, which, according to the arguments presented above, should be delocalized over the entire ZrN≡NZr subunit.

Both terminal and bridging dinitrogen ligands coordinated to the same metal appear to be a feature unique to $\{(\eta^5\text{-}C_5Me_5)_2ZrN_2\}_2N_2$. There do exist, however, a number of examples where a comparison can be made between a monomeric

Table VIII. Comparison of NN Bond Lengths and Stretching Frequencies for Monomeric and Analogus Binuclear Dinitrogen Complexes

Complex	Electronic configuration	ν(NN), cm^{-1}	d(NN), Å	Ref
$[(NH_3)_5RuN{\equiv}N]^{2+}$	d^6	2130	1.12 (8)	39, 40
$[(NH_3)_5RuN{\equiv}NRu(NH_3)_5]^{4+}$	d^6, d^6	2100 (Raman)	1.124 (15)	41–43
$(\eta^6\text{-}C_6H_5CH_3)(PPh_3)_2MoN{\equiv}N$	d^6	1988		44
$(\eta^6\text{-}C_6H_6)(PPh_3)_2MoN{\equiv}NMo(PPh_3)_2(\eta^6\text{-}C_6H_6)$	d^6, d^6	1910 (Raman)		44, 45
$\{(\eta^6\text{-}C_6H_5CH_3)(PPh_3)_2MoN{\equiv}NFe(Me_2PCH_2CH_2PMe_2)(\eta^5\text{-}C_5H_5)\}^+$	d^6, d^6	1930		44
trans-$[(PMe_2Ph)_4ClReN{\equiv}N]$	d^6	1925	1.055 (30)	46, 47
trans-$[(PMe_2Ph)_4ClReN{\equiv}NCrCl_3(THF)_2]$	d^6, d^3	1890		48, 49
trans-$[(PMe_2Ph)_4ClReN{\equiv}NMoCl_4(OMe)]$	d^6, d^1	1660	1.21	48, 50
trans-$[(PMe_2Ph)_4ClReN{\equiv}NZrCl_4]$	d^6, d^0	1790		48
trans-$[(PMe_2Ph)_4ClReN{\equiv}NAlEt_3]$	d^6	1890		48

complex containing a terminal N_2 and the analogous binuclear complex in which N_2 bridges two metal centers, at least one of which is identical with the monomeric metal fragment (Table VIII). A comparison of $[(NH_3)_5RuN{\equiv}N]^{2+}$ to $[(NH_3)_5RuN{\equiv}NRu(NH_3)_5]^{4+}$ reveals that coordination of a second $[(NH_3)_5Ru]^{2+}$ fragment to the terminal N_2 of the monomer results in only a minor reduction in N-N bond order. Similarly, coordination of a second Mo(0) or Fe(II) d^6 metal center to the terminal N_2 of (η^6-arene)$(PPh_3)_2MoN{\equiv}N$ leads to a relatively small reduction of the N-N stretching frequency. The large shift to lower energy of the ν (NN) band and a large increase in N-N bond length observed upon complexation of $MoCl_4(OCH_3)$ to *trans*-$[(PMe_2Ph)_4ClReN{\equiv}N]$ stands in sharp contrast, however.

As first suggested by Chatt[46,47] and co-workers and later restated by Sellman,[1] the relationship between the d-electron configuration of the acceptor metal atom bound to the free end of the dinitrogen ligand and the extent of N≡N bond reduction may be understood qualitatively in terms of four center π-molecular orbitals spanning both metals via the μ-N_2 π system (Figure 8). A major factor governing the strengths of the M-N and N-N bonds are the occupancies of the 2e and 3e levels. Population of the 2e level (π^* N_2 in character) will result in a marked reduction in N-N bond order, whereas population of 3e (π N_2 in character) will increase the N-N bond strength. Thus in the cases for which *both* M and M′ possess formal d^6 configurations (e.g., $[(NH_3)_5Ru$-$N{\equiv}NRu(NH_3)_5]^{4+}$), both 2e and 3e levels are occupied and little net reduction in N-N bond order beyond that for the monomer is achieved. On the other hand, when M′ possesses two d electrons (which may be placed in the d_{xy} δ-type orbital) or less, only the 2e level is occupied, and a marked reduction in N-N bond order results (e.g., *trans*-$[(PMe_2Ph)_4$-$ClReN{\equiv}NMoCl_4(OCH_3)]$). Alternatively, we note that the presence of *empty* acceptor metal (M′) d orbitals of proper symmetry for interaction with the μ-N_2 π orbitals enhances the donor metal (M)-to-N_2 π interaction, thereby increasing the M-N_2 and M′-N_2 bonding and decreasing the μ-N≡N bond order. The resulting situation may be viewed as a type of "push-pull" π bonding with substantial polarization of the MN≡NM′ unit.

$\{(\eta^5\text{-}C_5Me_5)_2ZrN_2\}_2N_2$ falls into this general class of binuclear complexes for which N_2 bridges a π-donor to a π-acceptor metal; however, it offers the added feature that the effect works in both directions. It is interesting to note that the intense visible absorptions observed for binuclear adducts of *trans*-$[(PMe_2Ph)_4ClReN_2]$ have been tentatively assigned to Re-to-M′ charge transfer.[49] We are presently investigating the possibility that at least one of the three intense bands (392, 544, 771 nm) exhibited by **1** are associated with Zr-to-Zr charge transfer.[51] Such facile charge transfer across the ZrN≡NZr unit may well play a deciding role in the HCl-promoted reduction of one N_2 to hydrazine.[10,52]

Acknowledgment. This work was supported by the National Science Foundation (Grant No. MPS 75-03056) and by Research Corporation, to whom grateful acknowledgment is made. We wish to thank Drs. Frank R. Fronczek and Neil S. Mandel for their efforts toward solving the structure. We are also most grateful to Drs. Joseph Lauher and Roald Hoffmann for supplying information prior to publication, and to Dr. W. A. Goddard for helpful discussions.

Supplementary Material Available: structure factor amplitudes (30 pages). Ordering information is given on any current masthead page.

References and Notes

(1) For recent reviews, see A. D. Allen, R. O. Harris, B. R. Loescher, J. R. Stevens, and R. N. Whiteley, *Chem. Rev.*, **73**, 11 (1973); D. Sellman, *Angew. Chem., Int. Ed. Engl.*, **13**, 639 (1974).
(2) E. E. van Tamelen, *Acc. Chem. Res.*, **3**, 361 (1970), and literature cited therein.
(3) (a) A. E. Shilov, A. K. Shilova, and E. F. Kvashina, *Kinet. Katal.*, **10**, 1402 (1969); (b) A. E. Shilov, E. F. Kvashina, and T. A. Vorontsolva, *Chem. Commun.*, 1590 (1971); (c) Y. G. Borod'ko, I. N. Ivleva, L. M. Kachapina, S. I. Salienko, A. K. Shilova, and A. E. Shilov, *J. Chem. Soc., Chem. Commun.*, 1178 (1972); (d) Y. G. Borod'ko, I. N. Ivleva, L. M. Kachapina, E. F. Kvashina, A. K. Shilova, and A. E. Shilov, *Ibid.*, 169 (1973).
(4) J. E. Bercaw, R. H. Marvich, L. G. Bell, and H. H. Brintzinger, *J. Am. Chem. Soc.*, **94**, 1219 (1972).
(5) C. Ungurenasu and E. Streba, *J. Inorg. Nucl. Chem.*, **34**, 3753 (1972).
(6) E. E. van Tamelen, W. Cretney, N. Klaentschi, and J. S. Miller, *J. Chem. Soc., Chem. Commun.*, 481 (1972).
(7) J. E. Bercaw and H. H. Brintzinger, *J. Am. Chem. Soc.*, **93**, 2046 (1971).
(8) J. E. Bercaw, E. Rosenberg, and J. D. Roberts, *J. Am. Chem. Soc.*, **96**, 612 (1974).
(9) J. E. Bercaw, *J. Am. Chem. Soc.*, **96**, 5087 (1974).
(10) J. M. Manriquez and J. E. Bercaw, *J. Am. Chem. Soc.*, **96**, 6229 (1974).
(11) R. D. Sanner, D. M. Duggan, T. C. McKenzie, R. E. Marsh, and J. E. Bercaw, *J. Am. Chem. Soc.*, following paper in this issue.
(12) D. J. Wehe, W. R. Busing, and H. A. Levy, Oak Ridge National Laboratory, Oak Ridge, Tenn., 1962, Report ORNL-TM-229.
(13) A. J. C. Wilson, *Nature (London)*, **150**, 151 (1942).
(14) D. T. Cromer and J. B. Mann, *Acta Crystallogr., Sect. A*, **24**, 321 (1968).
(15) C. H. Wei, *Inorg. Chem.*, **8**, 2384 (1969).
(16) A. C. Larson, *Acta Crystallogr.*, **23**, 664 (1967).
(17) D. J. Duchamp, American Crystallograhic Association, Bozeman, Montana, 1964, Paper B-14.
(18) The standard deviation given in parentheses following an average bond distance or angle, $\bar{x}$, is defined as:

$$\sigma = [\textstyle\sum_i (x_i - \bar{x})^2/(N-1)]^{1/2}$$

where N is the number of observations, x_i.
(19) M. A. Busch and G. A. Sim, *J. Chem. Soc. A*, 2225 (1971).
(20) K. W. Muir, *J. Chem. Soc. A*, 2663 (1971).
(21) E. F. Epstein, I. Bernal, and H. Köpf, *J. Organomet. Chem.*, **26**, 229 (1971).
(22) J. L. Calderon, F. A. Cotton, B. G. DeBoer, and J. Takats, *J. Am. Chem. Soc.*, **93**, 3592 (1971).
(23) V. V. Tkachev and L. O. Atovinyan, *J. Struct. Chem. USSR*, **13**, 262 (1972); A. Clearfield, D. K. Warner, C. H. Saldarriaga-Molina, R. Ropal, and I. Bernal, *Can. J. Chem.*, **53**, 1622 (1975).
(24) T. C. McKenzie, R. D. Sanner, and J. E. Bercaw, *J. Organomet. Chem.*, **102**, 457 (1975).
(25) I. A. Ronova, N. V. Alekseev, N. V. Gapotchenko, and Y. T. Struchkov, *J. Organomet. Chem.*, **25**, 149 (1971).
(26) J. J. Stezowski and H. A. Rick, *J. Am. Chem. Soc.*, **91**, 2890 (1969).
(27) M. Elder, *Inorg. Chem.*, **8**, 2103 (1969).
(28) D. C. Bradley, M. B. Hursthouse, and I. F. Rendall, *Chem. Commun.*, 368 (1970).
(29) J. L. Hoard, E. W. Silverton, and J. V. Silverton, *J. Am. Chem. Soc.*, **90**, 2300 (1968).
(30) A. A. Kossiakoff, R. H. Wood, and J. L. Burmeister, private communication.
(31) C. Ballhausen and J. P. Dahl, *Acta Chem. Scand.*, **15**, 133 (1961).
(32) N. W. Alcock, *J. Chem. Soc A*, 2001 (1967).
(33) J. C. Green, M. L. H. Green, and C. K. Prout, *J. Chem. Soc., Chem. Commun.*, **30**, 373 (1972).
(34) H. H. Brintzinger and L. S. Bartell, *J. Am. Chem. Soc.*, **92**, 1105 (1970).
(35) A. J. Petersen and L. F. Dahl, *J. Am. Chem. Soc.*, **96**, 2248 (1974).
(36) J. W. Lauher and R. Hoffmann, *J. Am. Chem. Soc.*, **98**, 1729 (1976).
(37) It is possible that if Zr–ring bonding is not weakened significantly, then the b_1 and a_2 orbitals may rehybridize such that one points more directly at the μ-N_2 π^* orbital.
(38) D. M. Duggan, J. M. Manriquez, and J. E. Bercaw, unpublished results.
(39) A. D. Allen, F. Bottomley, R. O. Harris, V. P. Reinsalu, and C. V. Saroff, *J. Am. Chem. Soc.*, **89**, 5595 (1967).
(40) F. Bottomley and S. C. Nyburg, *Acta Crystallogr., Sect. B*, **24**, 1289 (1968).
(41) D. E. Harrison, H. Taube, and E. Weissberger, *Science*, **159**, 320 (1968).
(42) J. Chatt, A. B. Nikolsky, R. L. Richards, and J. R. Sanders, *Chem. Commun.*, 154 (1969).
(43) I. M. Treitel, M. T. Flood, R. E. Marsh, and H. B. Gray, *J. Am. Chem. Soc.*, **91**, 6512 (1969).
(44) M. L. H. Green and W. E. Silverthorn, *J. Chem. Soc., Dalton Trans.*, 301 (1973).
(45) M. L. Green and W. E. Silverthorn, *Chem. Commun.*, 577 (1971).
(46) J. Chatt, J. R. Dilworth, and G. J. Leigh, *Chem. Commun.*, 687 (1969).
(47) B. R. Davis and J. A. Ibers, *Inorg. Chem.*, **10**, 578 (1971).
(48) J. Chatt, J. R. Dilworth, G. J. Leigh, and R. L. Richards, *Chem. Commun.*, 955 (1970).
(49) J. Chatt, R. C. Fay, and R. L. Richards, *J. Chem. Soc. A*, 702 (1971).
(50) M. Mercer, R. H. Crabtree, and R. L. Richards, *J. Chem. Soc., Chem. Commun.*, 808 (1973).
(51) D. M. Duggan, M. Burke, T. G. Spiro, and J. E. Bercaw, unpublished results.
(52) J. M. Manriquez, R. D. Sanner, R. E. Marsh, and J. E. Bercaw, *J. Am. Chem. Soc.*, **98**, 3042 (1976).